Third International Conference on Inverse Design Concepts and Optimization in Engineering Sciences (ICIDES-III), Editor: G.S. Dulikravich, Washington D.C., October 23-25, 1991.

INVERSE AIRFOIL DESIGN PROCEDURE USING A MULTIGRID NAVIER-STOKES METHOD

N92-13932
p. 12

by

J. B. Malone
Unsteady Aerodynamics Branch
Structural Dynamics Division
NASA Langley Research Center
Hampton, Virgina 23665–5225

and

R. C. Swanson
Theoretical Flow Physics Branch
Fluid Mechanics Division
NASA Langley Research Center
Hampton, Virgina 23665–5225

ABSTRACT

The Modified Garabedian-McFadden (MGM) design procedure was incorporated into an existing 2D multigrid Navier-Stokes airfoil analysis method. The resulting design method is an iterative procedure based on a residual-correction algorithm and permits the automated design of airfoil sections with prescribed surface pressure distributions. The new design method, MG-MGM, is demonstrated for several different transonic pressure distributions obtained from both symmetric and cambered airfoil shapes. The airfoil profiles generated with the MG-MGM code are compared to the original configurations to assess the capabilities of the inverse design method.

INTRODUCTION

The aerodynamic design of aircraft components is often carried out by means of one of the following four approaches: a) cut-and-try analysis, b) indirect methods, c) optimization techniques, and d) inverse design techniques. Unlike the cut-and-try method, the latter three design techniques are far more automated, and can significantly reduce the overall engineering effort and calendar time required for developing aircraft components and configurations with improved aerodynamic performance or aerodynamic interference characteristics.

A common design approach is to specify, a priori, surface pressure distributions that have favorable aerodynamic characteristics at given freestream conditions. For example, an appropriately chosen pressure distribution can be used to achieve certain desired lift and moment coefficient goals, while a "weak-shock" or "shock-free" distribution can be used to minimize wave drag performance penalties. The automated design procedure is then used to generate, as efficiently as possible, the configuration geometry which will cause the specified pressures to exist on the

designed component. Obviously, the use of these automated design methods requires that the aerodynamicist can specify, a priori, the desired pressure distributions for a particular application.

The most widely used aerodynamic design procedures for transonic-flow applications seem to be based upon potential-flow Computational Fluid Dynamics (CFD) methods.[1–5] This trend is most likely due to the relative low cost, in terms of computer-resource requirements, that is demonstrated by CFD methods based on the Transonic Small Disturbance (TSD) equation or the Full Potential equation (FPE). In the past decade, however, considerable interest has been demonstrated in the use of higher-order CFD methods such as the Euler equations and the Reynolds-averaged Navier-Stokes equations (RANS) for aerodynamic analyses in a variety of applications. Thus, there is now an increasing interest in also developing design procedures based on these higher-order CFD formulations.[6–10] If used during the design process, these higher-order CFD methods will help the aerodynamicist to account for the occurrence of fluid dynamic effects or phenomena which are not routinely predictable using potential flow methods.

In reference 11, Garabedian and McFadden described an inverse aerodynamic design procedure which they demonstrated using an existing FPE aerodynamics code. Their design method is based on a residual-correction algorithm, which we will refer to here as the GM method, and can be used to generate aerodynamic surfaces with prescribed surface pressure distributions. In reference 12, Malone, et al. presented a Modified Garabedian McFadden (MGM) design algorithm that removed some limitations of the original GM technique. These authors applied the new MGM design method, also using FPE aerodynamic analysis codes as a basis, to airfoil, axisymmetric nacelle inlet, and 3–D nacelle inlet design problems. Later, Hazarika[13] and Sankar used a FPE CFD method to apply the MGM procedure to the design of blended wing-body configurations. In a recent effort, Malone, et al.[14] described the first use of the MGM residual-correction design algorithm coupled with a 2–D Navier-Stokes solution procedure. Subsequently, a similar viscous-flow design procedure using MGM was presented by Birckelbaw[15], and new applications of MGM to multi-element airfoils using unstructured grids are under development.[16]

The objective of the present research was to develop an accurate design method for viscous, attached-flow, design problems which might be beyond the capability of potential-flow or Euler methods, even those using interactive boundary-layer theories. Because the aerodynamic designer normally seeks attached flow conditions, the method to be described is not expected to handle separated flow design problems. However, by virtue of the fact that a Navier-Stokes method forms the basis of the present procedure, the possible occurrence and extent of separated flow regions can be directly computed and noted by the designer during the design process.

The following sections of this paper will describe the multigrid Navier-Stokes computational procedure, the MGM design algorithm, implementation of the design procedure, and will also present the results of several sample airfoil design problems.

NAVIER-STOKES SOLUTION PROCEDURE

The two-dimensional Navier-Stokes procedure used in the present work was originally developed by Swanson and Turkel.[17] Their method solves the Reynolds-averaged form of the full Navier-Stokes equations (neglecting body forces and heat sources) on a body-fitted computational grid. The mathematical formulation in generalized coordinates consists of a non-dimensionalized

Third International Conference on Inverse Design Concepts and Optimization in Engineering Sciences (ICIDES-III), Editor: G.S. Dulikravich, Washington D.C., October 23-25, 1991.

set of equations cast in a strong conservative form:

$$Q_t + D_\xi + E_\eta = \sqrt{\gamma} M_\infty Re_c^{-1} (G_\xi + H_\eta) \tag{1}$$

In Eq. (1), Q is the vector of conserved flow variables, which are themselves combinations of the usual primitive variables, density (ρ), the components of fluid velocity (u, v), and the fluid total energy (e). The quantity M_∞ is the freestream Mach number and, Re_c is the Reynolds number. The vectors D and E are the inviscid flux vectors in the ξ and η coordinate directions, respectively. Also, the vectors G and H are the viscous flux terms in the corresponding coordinate directions. The techniques used to solve Eq. (1) are given in Refs. 17, 18, and 19. Here we present only a brief description of the Navier-Stokes solution procedure.

The spatial derivatives in the time-dependent Navier-Stokes equations are approximated with central differences. A cell-centered finite-volume technique is used to obtain the spatial discretization. For sufficiently smooth meshes the discretizations are second-order accurate. Adaptive numerical dissipation terms are appended to the resulting semidiscrete formulation. These terms, which are a blending of second and fourth differences, are included to provide shock capturing capability and to give the necessary background dissipation for convergence. In smooth regions of a flow field the dissipation terms are third order. The semidiscrete equations are integrated in time with a modified five stage explicit Runge-Kutta scheme. On the first, third, and fifth stages there is a weighted evaluation of the dissipation terms, which results in a good parabolic stability limit. The physical diffusion terms are evaluated only on the first stage and frozen for the remaining stages, without compromising stability. The decoupling of the temporal and spatial discretization makes the scheme amenable to convergence acceleration techniques, which are very beneficial in the computation of steady flows.

Three techniques are employed to accelerate convergence to steady state. The first one is local time-stepping, where the solution at any point in the domain is advanced at the maximum time step allowed by stability. This results in faster signal propagation, and thus, faster convergence. The second technique is variable coefficient implicit residual smoothing. It can be regarded as simply a mathematical step applied after each Runge-Kutta stage to extend the local stability range. The third technique is multigrid. A multigrid method involves the application of a sequence of meshes to a discrete problem to accelerate convergence of the time-stepping scheme. Successively coarser meshes can be generated by starting with the desired fine mesh and eliminating every other mesh line in each coordinate direction. An equivalent fine grid problem is defined on each coarse grid. Appropriate operators are introduced to transfer information between the meshes. In the method applied here a fixed W-type cycle is used to execute the multigrid strategy. The efficiency of the multigrid process depends strongly upon effective high frequency damping characteristics of the driving scheme. Such damping behavior is provided by the five stage Runge-Kutta scheme. The good smoothing of the highest frequencies on the coarser meshes allows rapid removal of the low frequency errors in the fine grid solution. There are two additional advantages of the multigrid method. First, less computational effort is required on the coarser meshes. Second, information is propagated faster on the coarser meshes due to larger allowable time steps.

Figure 1 presents typical computed lifts and moments for an NACA 0012 airfoil to demonstrate the capability of the multigrid algorithm for aerodynamic analysis applications. Turbulence closure was obtained with the Baldwin -Lomax model.

Third International Conference on Inverse Design Concepts and Optimization in Engineering Sciences (ICIDES-III), Editor: G.S. Dulikravich, Washington D.C., October 23-25, 1991.

MGM DESIGN PROCEDURE

The MGM design method can be classified as a residual-correction technique, in which the residuals are the difference between the desired speed distribution and the computed distribution. Over the past decade a number of residual-correction methods have been developed, such as the "wavy-wall" approach of Davis.[20] The methods differ primarily in the manner in which changes in residual are related to changes in surface shape. The MGM algorithm itself consists of an auxiliary PDE that is solved for incremental changes in surface coordinates during each design cycle. The final aerodynamic shape is approached in a stepwise fashion through a cyclical iteration between the flow solver and the MGM algorithm.

Mathematical Formulation

The MGM auxiliary PDE is heuristic in derivation and assumes that changes in surface pressures are proportional to changes in airfoil surface slopes and curvatures. For two-dimensional flow about an airfoil configuration, the auxiliary equation is given by

$$F_0 S_t + F_1 S_{xt} + F_2 S_{xxt} = R \tag{2}$$

where R is the residual, defined as $R = q_c^2 - q_t^2$. The quantities q_c and q_t are the computed and target speed distributions, the coordinate x is the usual cartesian coordinate taken here to lie along the airfoil chordline, and the coefficients F_0, F_1, and F_2 are constants chosen to provide a stable iterative process. Figure 2 shows how this auxiliary equation is typically incorporated into existing flow solution procedures. The computed surface velocities are normally obtained from partially converged numerical solutions to the flow equations under consideration at a given value of time, t. During the design process, as q_c approaches q_t, the right-hand side of Eq. (2) is reduced, and subsequent solutions of the auxiliary equation yield minimal changes in the airfoil surface coordinates.

Next, Eq. (2) is written in terms of a correction to the airfoil coordinates, ΔS, by using the temporal derivatives and choosing $\Delta t = 1$, so that Eq. (2) can then be written as:

$$F_0 \Delta S + F_1 (\Delta S)_x + F_2 (\Delta S)_{xx} = R \tag{3}$$

Numerical Solution Procedure

The auxiliary PDE is solved by writing finite-difference expressions for each term of Eq. (3). The computational grid used to solve this equation is the same grid used for the fluid-dynamic equations, which for the present Navier-Stokes solver, is an algebraically generated C-grid topology. Equation (3) is solved only along the airfoil surface, so that only the grid-line clustering in the x or streamwise direction is of importance.

Assuming that there are a total of N computational points on the airfoil surface, Eq. (3) is written for each of these points, i, where $1 \leq i \leq N$. A typical equation evaluated at the i th point on the surface is

$$A_i \Delta Y_{i+1} + B_i \Delta Y_i + C_i \Delta Y_{i-1} = R_i \tag{4}$$

The coefficients A_i, B_i, and C_i are evaluated by means of standard finite difference expressions, and ΔY_i is the incremental change in surface coordinate, ΔS, at the i th computational point. Equation (4) is evaluated at each point, i, around the airfoil surface, leading to a system of equations with N unknowns, the ΔY_i values. At each point on the aerodynamic surface, ΔY_i is coupled to values at each neighboring point. The resulting algebraic equations form a tridiagonal system that is solved for values of ΔY_i using the Thomas algorithm.[21]

The design cycle is completed by updating the previous surface geometry using the new values of ΔY_i as follows:

$$Y_i^{new} = Y_i^{old} + \Delta Y_i, \; for \; i = 1 \; to \; N \tag{5}$$

Additional details of the MGM algorithm can be found in References 12 and 14.

Trailing-Edge Crossover

The present inverse procedure was developed to permit the design of complete airfoil surfaces, including the leading-edge and trailing-edge regions. However, a completely arbitrary choice for a target pressure distribution does not always result in a well-posed inverse design problem. For example, Volpe[4] has presented a technique to satisfy the three integral constraints relating target pressures and freestream conditions that are required to insure a well-posed problem in compressible flow. As a possible consequence of using unconstrained target pressures, any inverse procedure may produce an airfoil geometry which may exhibit trailing-edge crossover, or lead to other unrealistic configurations.

Therefore an artifice is used in the present work so that the trailing edge thickness can be controlled and so that any tendency of the airfoil to "fish-tail" is identified. If the geometry is driven to a "fish-tail" configuration (trailing-edge crossover), a linear wedge is added to the airfoil section so that the resulting trailing-edge thickness equals a predetermined value. It has been demonstrated that this wedge technique can give some measure of control over the potential manufacturability of airfoil configurations generated by automated design procedures.[22] It should be noted that if the above wedging technique is required continuously during the design process, the original target pressures should be examined for possible modification along the lines discussed by Volpe[4]. A technique such as this may be used to modify these pressure distributions in order to rigorously provide for a well posed inverse design problem.

RESULTS

The MGM design procedure has been incorporated into the 2–D Navier-Stokes code described previously. The resulting computer program is referred to here as the MG-MGM code. In this section, we present three sample problems to illustrate application of the design method. Target pressures are obtained from a known "target geometry", and the inverse design method is then used to "reproduce" the original "target" configuration. These test cases demonstrate that the starting geometry, or baseline configuration, used to start the design process does not have to be "close" in thickness or camber to the target geometry.

Several parameters were held constant for each of the sample problems. A "W-type" multigrid cycle was used throughout, together with five successive levels of grid refinement. Also, five "W"multigrid cycles were used between all airfoil geometry updates (ie. one design cycle). The computational C-grid used consisted of 321 nodes in the wrap-around, or ξ-direction (33 of these in the wake region) and 64 nodes in the surface-normal, or η−direction, for a total of 20,544 grid points. The first η = constant grid line was clustered to within 0.0001 chord lengths from the airfoil surface. Since each point on the airfoil surface is allowed to move independently, each can be thought of as an independent variable in the context of an optimization problem. For the cases presented above, there were 257 such points around the airfoil surface.

For each case presented, a total of 160 design cycles (i.e. geometry updates) were specified. The program was executed on a Cray 2 and each airfoil design required approximately 16 minutes of CPU. Comparable Euler designs would require approximately 11 minutes on the same machine for a similarly dimensioned grid.

Design Case No. 1

For Case No. 1, the MG-MGM code was first used in the analysis mode to compute the surface pressures corresponding to an RAE 2822 airfoil at M_∞ = 0.8, an angle of attack, α, equal to zero degrees, and Re_c = 6,500,000, based on airfoil chord.

This calculated C_p distribution was then used as a target distribution for the MG-MGM code operated in the design mode. The baseline airfoil used to start the design was an NACA 0012 section. As shown in Fig. 3, this airfoil is significantly different in shape from the RAE 2822 airfoil used to produce the target pressure distribution. In this figure, as well as others depicting airfoil geometry, the vertical scale has been expanded.

Figure 4 compares the design and target airfoil pressures after 40 design cycles while Fig. 5 compares the design and target airfoil contours at this point in the design process. Figures 6 and 7 present the corresponding comparisons for pressure and geometry after 160 design cycles. Figure 8 shows the results of a separate analysis computation performed after the design was completed. This analysis started from uniform freestream conditions (impulsive start) and used the grid produced by the designed airfoil contour given in Fig. 7. The comparison between design and target pressures is actually better than that observed during the design process. This better correlation exists because the pressures obtained during the design process are generated with only a small number of multigrid cycles on the latest computational grid. The final design corresponds to 160 updates to the airfoil geometry and 160 grid-generation steps. The MGM design algorithm itself is not computationally intensive, and because a simple algebraic grid generation scheme is also used in the present application, the computational overhead represents only a small fractional increase over that which would be required to run the original CFD method in the analysis mode.

Design Case No. 2

For Case No. 2, the MG-MGM code was used in the analysis mode to compute the surface pressures corresponding to an NACA 0012 airfoil at M_∞ = 0.8, an angle of attack, α = 2.0 degrees, and Re_c = 6,500,000, based on airfoil chord.

This calculated C_p distribution was again used as a target distribution for the MG-MGM code operated in the design mode. This time the baseline airfoil was also an NACA 0012 section.

However, during the design process, the freestream angle of attack was kept at α = 0.0 degrees. This case was used to study the possible effects that a mismatch between specified pressures and angle of attack might have on the design process. Figure 9 compares the baseline and target airfoil pressures for this case. As would be expected for a transonic flight condition, the shock wave locations are significantly different for the α = 2.0 targets and the α = 0.0 baseline condition.

Figure 10 compares the design and target airfoil pressures after 40 design cycles, while Fig. 11 compares the design and target airfoil contours at this point in the design process. As can be seen in Fig. 11, after 40 design cycles the airfoil surface has already been rotated upwards to adjust to the target pressure. Figure 12 presents a comparison of the geometry after 160 design cycles. As in the previous case, a separate analysis run was performed to verify the airfoil design. Figure 13 shows the results of the separate analysis computation performed after the design was completed. This analysis started from uniform freestream conditions (impulsive start) and used the grid produced by the designed airfoil contour given in Fig. 12. Finally Fig. 14 shows a plot of the average Δq^2 versus multigrid work for the 800 multigrid cycles. This quantity drops approximately two orders of magnitude during the design process and is used to monitor the progress of the design algorithm.

Design Case No. 3

The final example problem, design Case No. 3, was chosen to demonstrate that large geometric changes can be achieved with the MGM design algorithm. For this application, the target pressures corresponded to an NACA 0012 airfoil at M_∞= 0.8, angle of attack, α = 0.0 degrees, and Re_c = 6,500,000, based on airfoil chord. The baseline configuration used was an NACA 0006 airfoil. A comparison of the target and final design airfoil shapes is shown in Fig. 15. A comparison of the target pressures, and those obtained from a separate analysis (impulsive start) of the final design configuration are shown in Fig. 16. In this example, an airfoil design was successfully accomplished which required a 100% increase in airfoil thickness over that of the baseline airfoil shape.

CONCLUDING REMARKS

The MGM design procedure has been incorporated into an existing multigrid Navier-Stokes code. The computational efficiency of the method indicates that it is a viable tool for the design process. The actual computational effort of this design method depends, of course, on the complexity of the target pressure distributions chosen. Normally, aerodynamicists would seek to eliminate shockwaves due to the impact of wave drag on performance. Previous experience with the MGM algorithm[14] indicates that shock-free design applications require about 50% less computational effort than for flows with shockwaves present. The transonic flow cases shown here were picked, in part, to demonstrate the design algorithm's robustness and ability to respond correctly to shockwaves in the flowfield. This feature is important because regions of sonic flow may be created locally near regions of high airfoil curvature even at relatively low freestream Mach numbers.

Because of the computer resource requirements, any Navier-Stokes based design method would likely be used in combination with other, lower-cost design methods. For example, an initial airfoil shape designed with a FPE method may prove to be an excellent starting configuration for

a higher-order design approach. Used in this manner, the present Navier-Stokes inverse design method should then be able to account for viscous flowfield phenomena that may not be detected or predicted accurately enough by other methods based on FPE or Euler solution procedures.

REFERENCES

1. Sloof, J. W.: Computational Methods for Subsonic and Transonic Aerodynamic Design, AGARD Report No. 712, 1983.

2. Lores, M. E.; and Smith, P. R.: Supercritical Wing Design Using Numerical Optimization and Comparisons with Experiment, AIAA Paper 79–0065, AIAA 17th Aerospace Sciences Meeting, New Orleans, LA, January 15–17, 1979.

3. Weed, R. A.; Anderson, W. K.; and Carlson, L. A.: A Direct-Inverse Three-Dimensional Transonic Wing Design Method for Vector Computers, AIAA Paper 84–2156, AIAA 2nd Applied Aerodynamics Conference, Seattle, WA, August 21–23, 1984.

4. Volpe, G: Inverse Design of Airfoil Contours: Constraints, Numerical Method, and Applications, Paper No. 2, AGARD Specialists Meeting on Computational Methods for Aerodynamic Design (Inverse) and Optimization, Loen, Norway, May 22–24, 1989.

5. Takanashi, S.: Iterative Three-Dimensional Transonic Wing Design Using Integral Equations, Journal of Aircraft, Vol. 22, No. 8, August 1985, pp. 655–660.

6. Mani, K. K.: Design Using Euler Equation, AIAA Paper 84–2166, AIAA 2nd Applied Aerodynamics Conference, Seattle, WA, August 21–23, 1984.

7. Giles, M. B.; and Drela, M.: Two-Dimensional Transonic Aerodynamic Design Method, AIAA Journal, Vol. 25, No. 9, September 1987, pp. 1199–1205.

8. Risk, M. H.: Applications of Single Cycle Optimization Approach to Aerodynamic Design, AIAA Paper 84–2165, AIAA 2nd Applied Aerodynamics Conference, Seattle, WA, August 21–23, 1984.

9. Hirose, N.; Takanashi, S.; and Kawai, N.: Transonic Airfoil Design Procedure Utilitizing a Navier-Stokes Analysis Code, AIAA Journal, Vol. 25, No. 3, March 1987, pp. 353–359.

10. Jameson, A.: Airfoil Design Via Control Theory, Paper No. 22, AGARD Specialists Meeting on Computational Methods for Aerodynamic Design (Inverse) and Optimization, Loen, Norway, May 22–24, 1989.

11. Garabedian, P.; and McFadden, G.: Design of Supercritical Swept Wings, AIAA Journal, Vol. 20, No. 3, March 1982, pp. 289–291.

12. Malone, J. B.; Vadyak, J.; and Sankar, L. N.: A Technique for the Inverse Aerodynamic Design of Nacelles and Wing Configurations, AIAA Paper 85–4096, Oct. 1985 (see also, Journal of Aircraft, Vol. 24, No. 1, January 1987, pp. 8–9.

13. Hazarika, N.: An Efficient Inverse Method for the Design of Blended Wing-Body Configurations, Ph.D. Thesis, Georgia Institute of Technology, June 1988.

14. Malone, J. B.; Narramore, J. C.; and Sankar, L. N.: An Efficient Airfoil Design Method Using the Navier-Stokes Equations, Paper No. 4, AGARD Specialists Meeting on Computational Methods for Aerodynamic Design (Inverse) and Optimization, Loen, Norway, May 22–24, 1989.

15. Birckelbaw, L.: Inverse Airfoil Design Using the Navier-Stokes Equations, AIAA Paper 89–2202, AIAA 7th Applied Aerodynamics Conference, Seattle, WA, July 31–August 2, 1989.

16. Jolly, B.: Private Communication, Wright Laboratories, WPAFB, January 1991.

17. Swanson, R. C.; and Turkel, E.: A Multistage Time-Stepping Scheme for the Navier-Stokes Equations, AIAA Paper 85–0035, AIAA 23rd Aerospace Sciences Meeting, Reno, NV, January 14–17, 1985.

18. Swanson, R. C.; and Turkel, E.: Artificial Dissipation and Central Difference Schemes for the Euler and Navier-Stokes Equations, AIAA Paper 87–1107, AIAA 8th Computational Fluid Dynamics Conference, Honolulu, HW, June 9–11, 1987.

19. Swanson, R. C.; and Radespiel, R.: Cell Centered and Cell Vertex Multigrid Schemes for the Navier-Stokes Equations, AIAA Journal, Vol. 29, No. 5, May 1991, pp. 697–703..

20. Davis, W. H.: Technique for Developing Design Tools from Analysis Methods of Computational Aerodynamics, AIAA Paper 79–1529, AIAA 12th Fluid and Plasma Dynamics Conference, Williamsburg, VA, July 23–25, 1979.

21. Anderson, D. A.; Tannehill, J. C.; and Pletcher, R. H.: Computational Fluid Mechanics and Heat Transfer, McGraw-Hill Book Company, 1984.

22. Malone, J. B.: Subsonic Panel Method for Iterative Design of Complex Aircraft Configurations, Journal of Aircraft, Vol. 19, No. 10, October 1981, pp. 820–825.

Third International Conference on Inverse Design Concepts and Optimization in Engineering Sciences
(ICIDES-III), Editor: G.S. Dulikravich, Washington D.C., October 23-25, 1991.

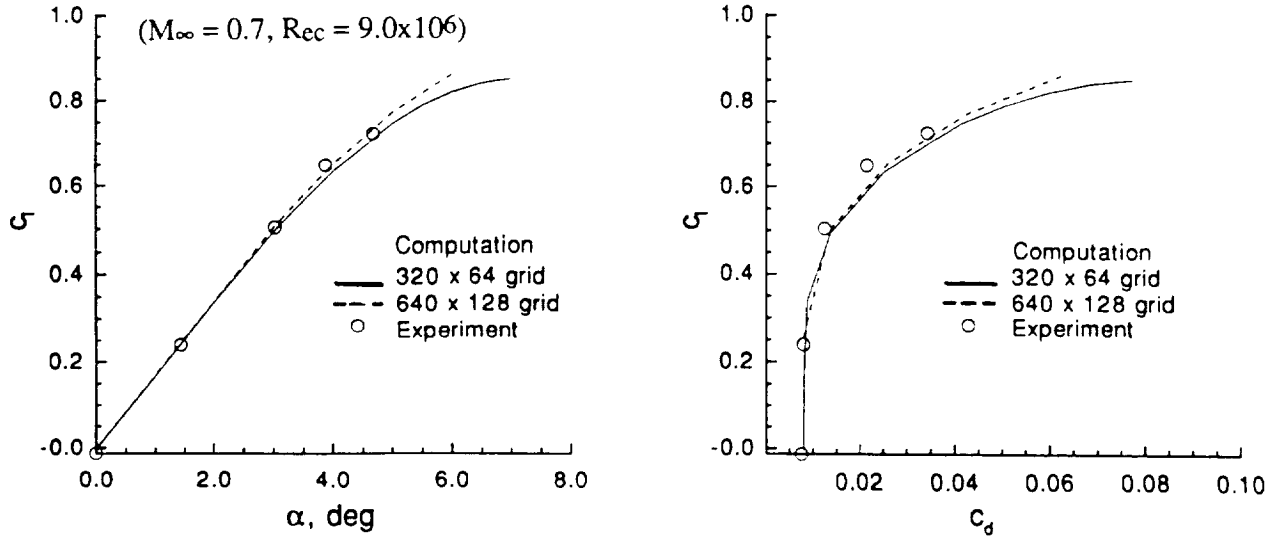

(a) Lift curve (b) Drag polar

Figure 1. Variation of lift and drag coefficients for NACA 0012 airfoil

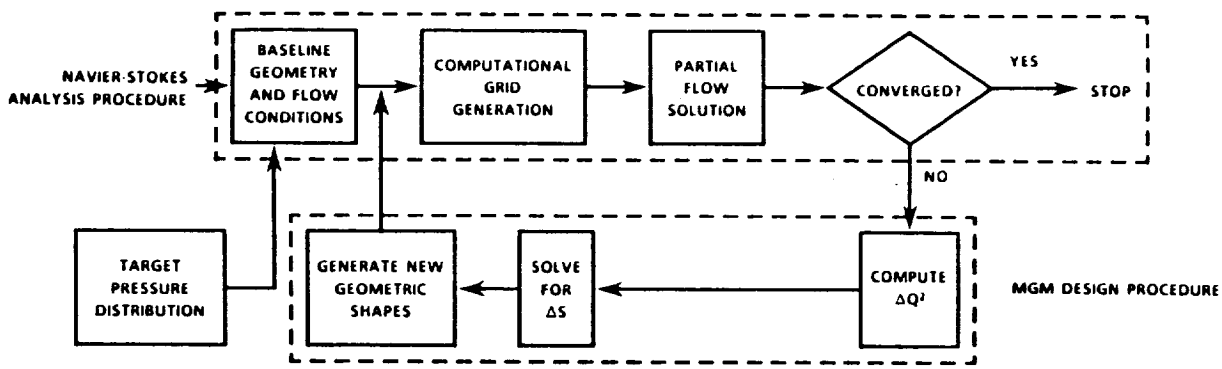

Figure 2. Implementation of the MGM Inverse Design Algorithm

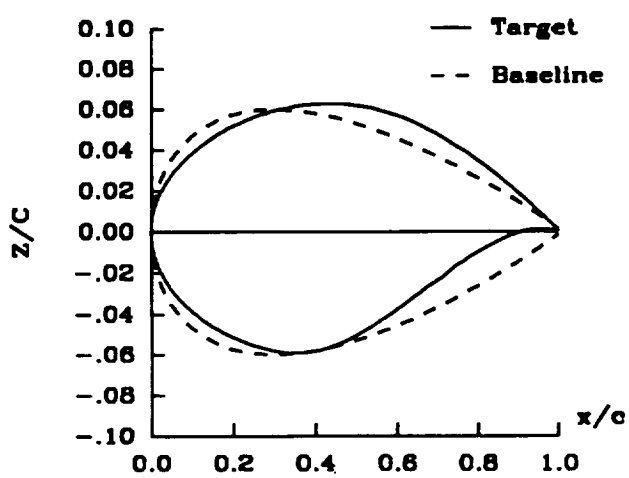

Figure 3. Comparison of target and baseline airfoil contours for case no. 1

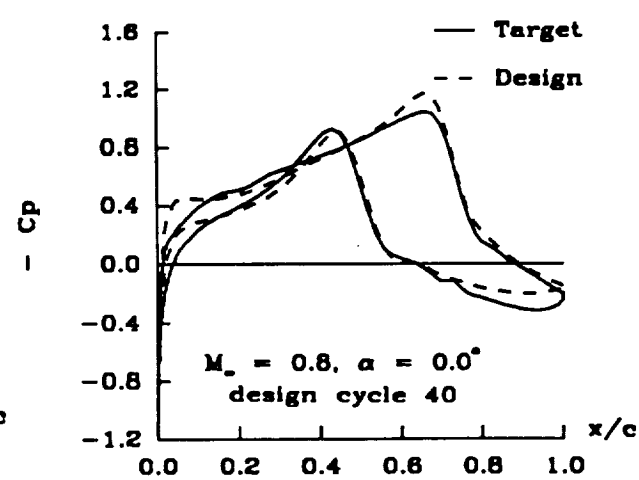

Figure 4. Comparison of target and inverse airfoil pressures for case no. 1

Third International Conference on Inverse Design Concepts and Optimization in Engineering Sciences (ICIDES-III), Editor: G.S. Dulikravich, Washington D.C., October 23-25, 1991.

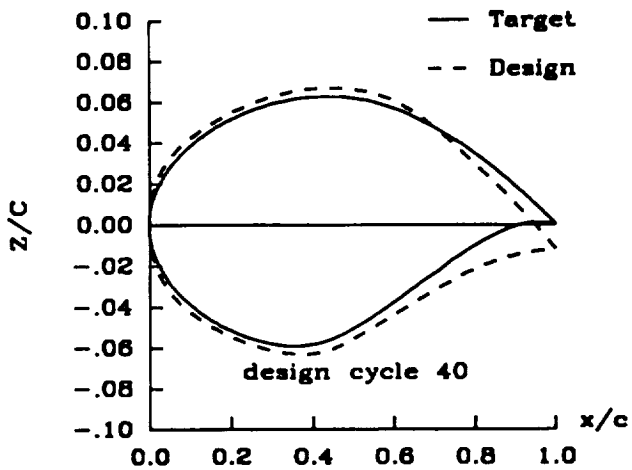

Figure 5. Comparison of target and inverse airfoil contours for case no. 1

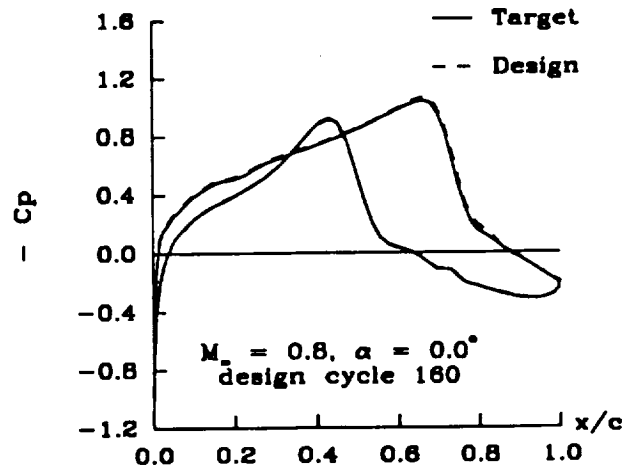

Figure 6. Comparison of target and inverse airfoil pressures for case no. 1

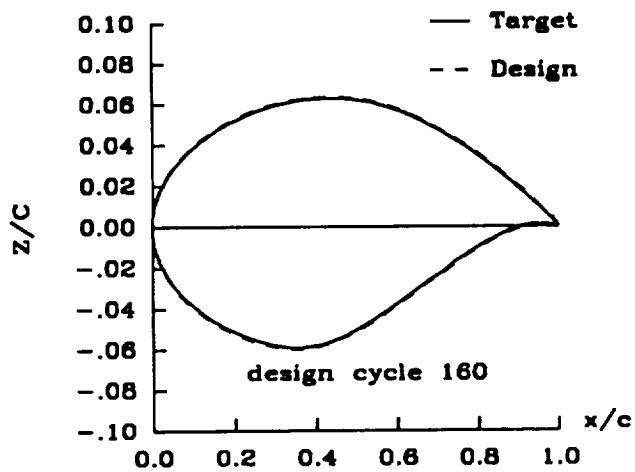

Figure 7. Comparison of target and inverse airfoil contours for case no. 1

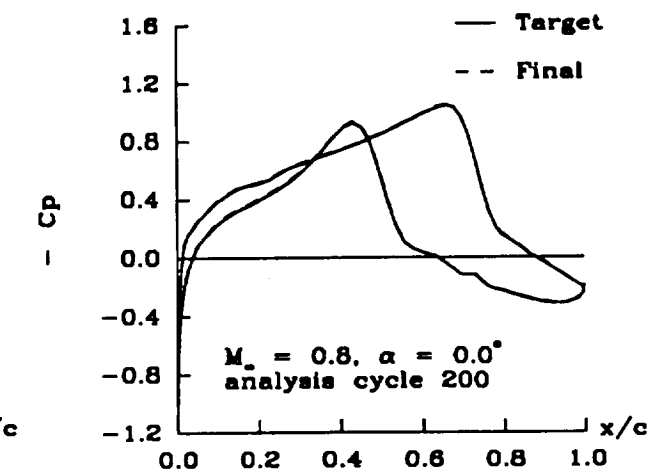

Figure 8. Comparison of target and final airfoil pressures for case no. 1

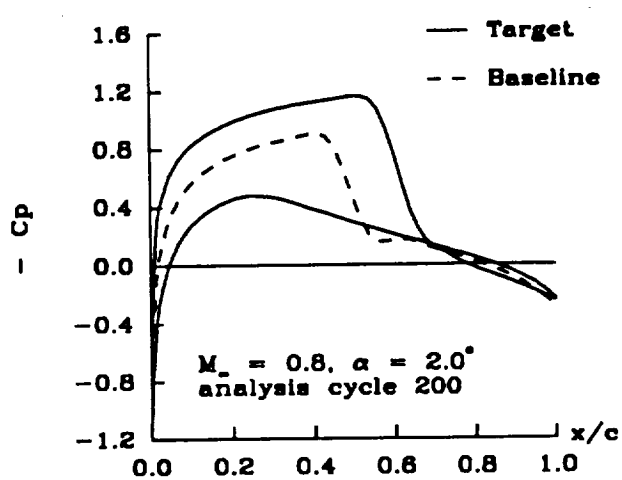

Figure 9. Comparison of target and baseline airfoil pressures for case no. 2

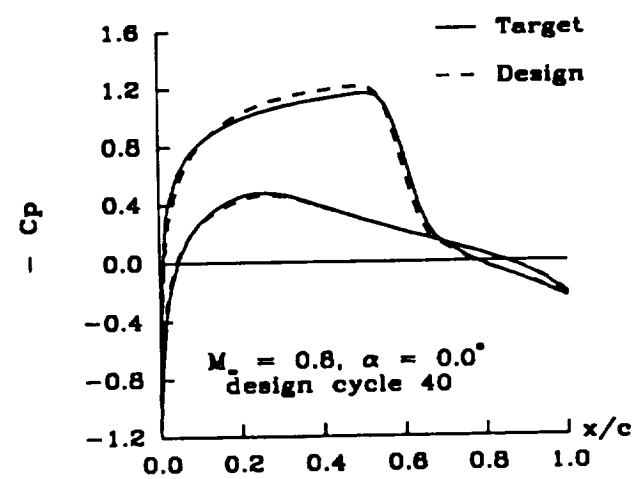

Figure 10. Comparison of target and inverse airfoil pressures for case no. 2

Third International Conference on Inverse Design Concepts and Optimization in Engineering Sciences
(ICIDES-III), Editor: G.S. Dulikravich, Washington D.C., October 23-25, 1991.

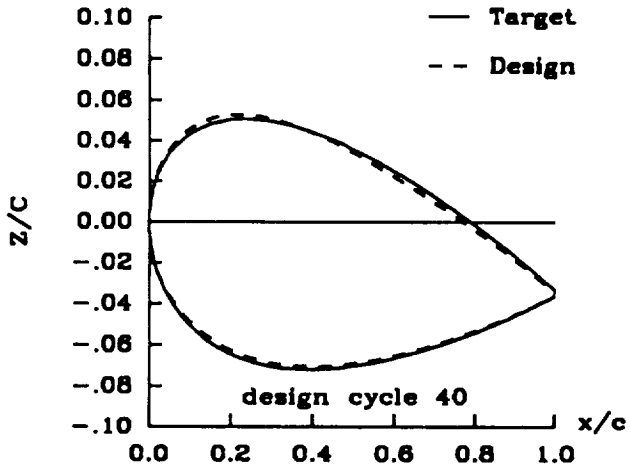

Figure 11. Comparison of target and inverse airfoil contours for case no. 2

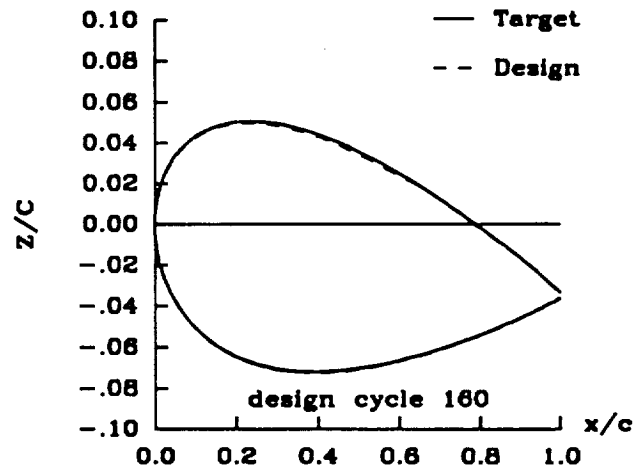

Figure 12. Comparison of target and inverse airfoil contours for case no. 2

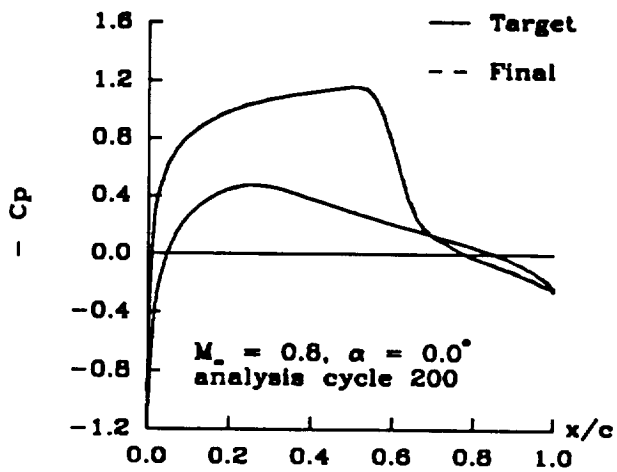

Figure 13. Comparison of target and final airfoil pressures for case no. 2

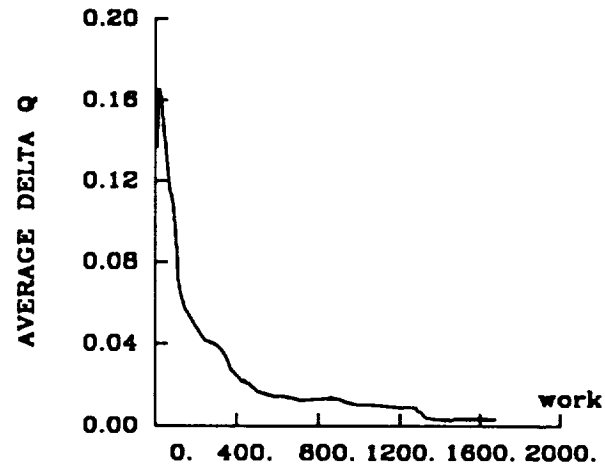

Figure 14. Average Δq^2 versus multigrid work performed for case no. 2

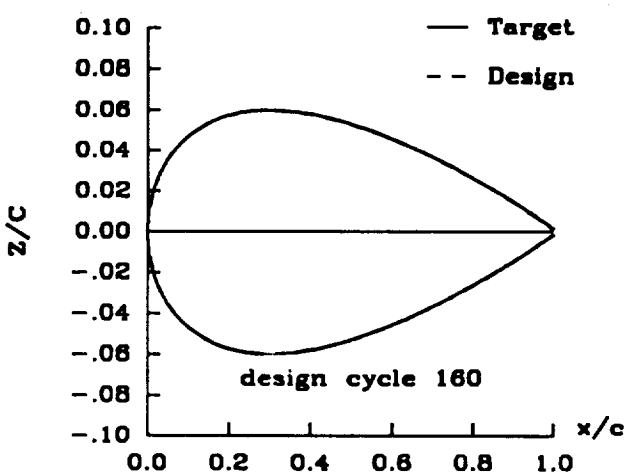

Figure 15. Comparison of target and inverse airfoil contours for case no. 3

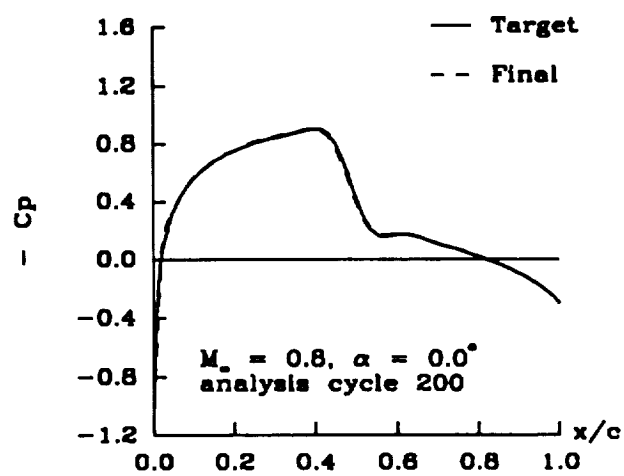

Figure 16. Comparison of target and final airfoil pressures for case no. 3